# An Approach to Estimate Emissivity For Thermography-based Material Recognition

Tamas Aujeszky
*Engineering Department*
*New York University Abu Dhabi*
Abu Dhabi, United Arab Emirates
tamas.aujeszky@nyu.edu

Georgios Korres
*Engineering Department*
*New York University Abu Dhabi*
Abu Dhabi, United Arab Emirates
george.korres@nyu.edu

Mohamad Eid
*Engineering Department*
*New York University Abu Dhabi*
Abu Dhabi, United Arab Emirates
mohamad.eid@nyu.edu

Farshad Khorrami
*Electrical and Computer Engineering Department*
*New York University*
Brooklyn, United States of America
khorrami@nyu.edu

***Abstract*—Multimodal characterization of unknown environments is of increasing necessity in various applications (such as autonomous or Tele-operated robots). While audiovisual mapping can be performed in high fidelity and real time, haptic mapping is lagging behind. Infrared thermography is an emergent technology for performing material characterization without a need for contact between the sensing element and the object, enabling a wider range of use cases, such as dealing with delicate items. However, the signal provided by a thermal camera used in such setups depends on the thermal emissivity of the examined sample. This paper presents an approach to estimate the emissivity of an object through its reflection of light. The contactless nature of this approach allows for it to be used as part of a thermographic material characterization framework.**

***Index Terms*—Thermography, Thermal radiation, Haptic interfaces**

## I. Introduction

There are many existing, new and upcoming scenarios in which a task to characterize an unknown environment is vital to carry out. Nowadays we can accurately and quickly capture audio, video and depth with state of the art cameras. However, the factors that create our sense of touch are not as effectively scanned or modeled yet. The common need for mapping haptic modality is either to equip machines with this skill (social/industrial robotics) or to simulate the experience for humans in environments where it would not naturally occur (teleoperation, telepresence, augmented/virtual reality). This would result in precise and accurate operation for robots and provide immersive and lifelike experience for humans.

There exist a few approaches to map the haptic properties by measuring their physical characteristics. Most of these approaches entail contact-based surface-tool interactions, which means that every single object would need to be contacted. This seems tedious regardless of whether it is performed in advance (such as when a scene is recorded to be used in a virtual environment) or on the fly (when a robot maps its surroundings), not to mention that some delicate objects might not react optimally to being subjected to a contact force. These considerations direct the attention of research towards a contactless mapping tool.

Our recent publications have proposed and demonstrated the suitability of infrared thermography for material characterization [1]–[3]. An overview of a thermographic material characterization framework is seen in Figure 1. Such a system studies the response of the material to being subjected to a slight thermal excitation. The temporal and spatial evolution of the thermal gradient on an object's surface enable the categorization of the material composition of the object, which in turn can help in determining its physical properties.

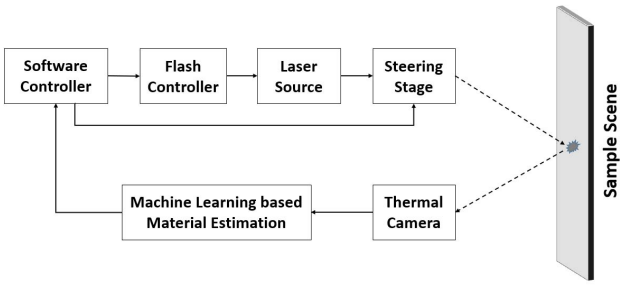


Fig. 1. Diagram of a thermographic material characterization framework

One of the fundamental challenges when it comes to using thermal cameras for quantitative evaluations is the estimation of thermal emissivity. Emissivity is the ratio of the amount of thermal radiation produced by an object compared to an otherwise identical perfect black body radiator [4]. These objects are governed by Planck's Law that describes the magnitude and spectral distribution of the radiation with respect to the temperature of the object. A thermography setup has to compensate for this scaling factor before it can deduce the temperature of the object from its radiation spectrum.

There are two established methods for measuring the emissivity of an object. One method relies on accurately measuring the temperature of the object, while another requires a tape

978-1-5386-8344-6/19/$31.00 ©2019 IEEE

with known emissivity value to be placed on the object and achieve perfect thermal contact with it [5], [6]. Neither of these methods permit the estimation of the emissivity of an object with unknown temperature in a contactless fashion.

This paper presents an alternative approach to estimate the emissivity of unknown objects. As light hits the surface, it is transmitted through the surface, absorbed by the surface or reflected from the surface. The sum of the intensities of transmitted, absorbed and reflected light are equal to that of the incident light and independent of the characteristics of the surface. The ratios of the intensity of transmitted, absorbed and reflected light compared to the incident light are transmittance, absorptance and reflectance, and their sum is consequently 1. Moreover, the transmittivity of opaque objects is assumed 0 for if they are sufficiently thick. The electromagnetic power absorbed by an object is equal to its emitted power at thermal equilibrium (Kirchhoff's law) [7]. Therefore its emissivity is equal to its absorptivity. Therefore, the sum of the ratio of reflected electromagnetic power to the incident power and the emissivity of the opaque object sums up to 1. This allows for the estimation of the emissivity of an object based on known power of incident light and measured power of reflected light.

The rest of this paper is organized as follows: Section 2 presents existing work in this field, while Section 3 describes the conducted experiment. The results are detailed in Section 4, and the discussion of results can be found in Section 5. Finally, conclusions are drawn in Section 6, along with stating our plans for future research.

## II. Related Work

This research topic lies at the intersection of multiple areas, including material characterization and recognition, haptic modeling, infrared thermography and emissivity measurement. There has been extensive research on material recognition based on visual information [8], [9]. These methods are certainly useful but there is a limitation in that different materials can have very similar visual properties (such as glossy white acrylic or glossy white silicone).

Another approach for acquiring information about materials is by characterizing contact interaction between a tool and the material surface, also known as tool-surface interaction. This can provide relevant and precise information about the object's physical properties by measuring values of position, velocity, acceleration, vibration, force or torque as a pen-shaped tool probes the surface of the object [10], [11]. While these measurements work well in general, they are intrinsically limited by a need for physical contact between the sensing tool and the object.

Infrared thermography as a technology has been around since the 1980s, and has largely been used for nondestructive testing and evaluation of materials in industry [12]–[15]. Despite its decades long application for acquiring information about materials, it has been mostly used for qualitative purposes, such as fault detection [16], [17], examination of various works of art [18], [19] and characterization of electronic circuits [20]–[22].

Quantitative thermographic analysis can reveal information about the physical properties of the material, such as thermal diffusivity [1], [24]–[27] and thermal emissivity [5], [6], [28]. Measuring or estimating the emissivity of a material with high precision is a difficult task. There are three common methods: first, by comparing the measured radiation to a known temperature value using a thermocouple attached to the object [5]. Second, by covering part of the object with high-emissivity coating and ensuring perfect thermal contact [6]. This region will behave as a black body and it can be compared against the rest of the object. The third, and most commonly used method involves using a look-up table of emissivity values based on the material composition of the object [28]. Unfortunately, neither of these methods are suitable for non-contact emissivity estimation for material characterization.

In [29], a method to employ thermography on a wedge-like region of an object is proposed. Light entering this region undergoes a series of reflections and as such, the overall absorptivity (and consequently, emissivity) of the region is close to 1. Thermal radiation from this region can be used to compare against the rest of the object to determine emissivity. Iino et al. [30] presented an experiment to measure the effects of changing the paint on the surface of automobiles on their emissivities. An interesting research is [31], where the authors present a neural network-based system to correct for atmospheric absorption in measured emissivity graphs which can happen outside of the long-wave infrared range (8-14 $\mu$m, $\approx$ 207-362K),

Due to the relatively few areas of utilization for quantitative thermography, the need to develop a method for emissivity estimation that is contactless and fast was never present. It is vital however, for thermography-based material characterization that are in development and as such, this work is an essential element to realize thermography-based haptic modeling.

## III. Experimental Setup and Methodology

The experimental setup consisted of the following parts: an array of 5 LED lights, a photo diode, various experimental samples as well as a control circuit and a desktop workstation. An image of the setup can be seen in Figure 2, while a schematic diagram of the experiment is presented in Figure 3.

The photo diode is a Marktech MTPD4400D-1.4 model, having a spectral sensitivity in the 190nm - 570 nm range, covering a short spectrum around the visible-UV border. The LED lights emit a light of wavelength 390nm, with a cumulative power consumption of 260 mW. The control circuit consists of an amplifier to increase the magnitude of the signal, an Arduino microcontroller that samples the signal at 12 ms period ($\sim$ 83Hz) and instructs a relay for turning on/off the power supplied to the LED lights. The LED lights, the photo diode and the amplifier circuit are all located on the same board, at a distance of 5cm from the sample under examination. The Arduino board is controlled from a desktop computer running MATLAB through a serial connection and it supplies the computer with the collected data.

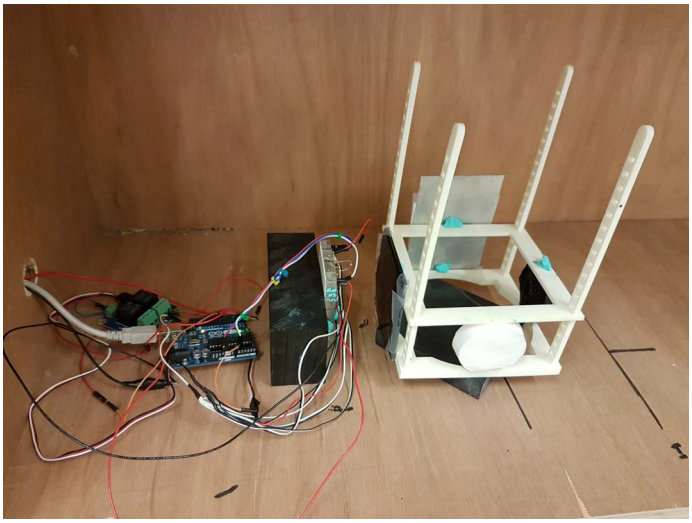

Fig. 2. Experimental setup.

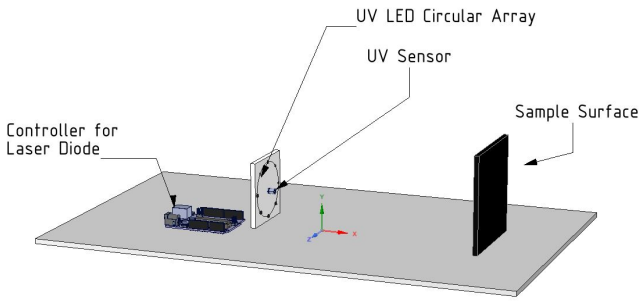


Fig. 3. Schematic diagram of the experimental setup.

The experimental samples are collected to create a 2x2x2 fully factorial design with respect to 3 parameters: color (black or white), finish (glossy or matte) and material (acrylic or silicone). An image of the samples can be seen in Figure 4. Each of these samples are fitted on a 3D-printed stand so that they are directly facing the LED lights and the photo diode.

Data acquisition is performed according to the following procedure: each of the experimental samples is examined for a total of 3 periods of data acquisition. Each of these periods begins with a 5 second pause. The LED lights are then turned on, and another 5 seconds later the Arduino board takes 1000 consecutive samples of the output of the amplifier. These 1000 samples span a time range of around 12 seconds.

## IV. Results

An example of the collected data can be seen in Figure 5. The data presented here is the voltage at the output of the amplification circuit, as sampled by the Arduino board. It can be seen that while the raw data has a large magnitude of additive noise, a moving average filter of length 11 drastically reduces the variance of the data.

All of the time-domain results can be seen in Figure 6, having subjected to smoothing by a moving average filter of length 11. These figures exemplify that all of the samples produce a consistent signal that does not increase or decrease with time or between different experimental runs.

It is clear from Figure 6 that black and white samples have a response that is radically different in magnitude, however there does not seem to be an immediate difference in material composition or finish. Given that our experimental design followed a fully factorial 2x2x2 arrangement, it seems logical to examine the three factors separately on all results. Figure 7 reflects these categories between acrylic and silicone, between glossy and matte, and between black and white, respectively.

Figure 8 displays the entirety of each categories as a separate box plot. Table I lists several statistical values for the different sample categories (acrylic, silicone, glossy, matte, black and white).

The average standard deviation per period (ASDPP) category refers to taking the standard deviation of the results of each data acquisition period (12 per sample category, with or without applying a moving average filter of length 11) separately, then averaging them. The cumulative average standard deviation (CASD) category refers to taking the signals of each category as a single signal and displaying its standard deviation (with or without applying the moving average filter).

It is clear that black and white results have a large difference. This is further emphasized by Table I, which lists the statistical characteristics for each of the categories. However, the other two pairs of categories demonstrate negligible differences: in both cases (acrylic versus silicone and glossy versus matte) the difference between the averages is less than 20% of the filtered standard deviations of these categories.

## V. Discussion

There are a couple of points worthy of discussion with respect to the results presented above. Firstly, the consistency of signals: as presented in Figure 5, the signal has a large magnitude of noise, but applying a moving average filter of 11 samples on it drastically reduces the variance of the noise (by around 80% in all cases, when taken as the average standard deviation per period). This means that capturing only 11 data points is sufficient to have highly reliable data on the sample under examination. This implies that the system is capable of performing data acquisition in around 132ms, which enables soft-real time emissivity estimation.

Looking at the differences between opposite categories, we can see the following: the black and white signals both have small cumulative average standard deviations (CASD) compared to their magnitudes, and this is reduced even further after filtering. Given that the black and white category means are significantly different, this means that the system clearly differentiates between objects of different color. Another observation is that the CASD values are not significantly higher than the ASDPP values. This means that taking all the different black samples and treating their signals as if they were produced by the same sample does not degrade the result by


Fig. 4. The samples used in the experiment.

TABLE I
RESULTS PER CATEGORY

| Category | Acrylic | Silicone | Glossy | Matte | Black | White |
|---|---|---|---|---|---|---|
| Mean | 273.0mV | 317.8mV | 301.2mV | 289.6mV | 75.7mV | 515.1mV |
| ASDPP | 113.9mV | 117.6mV | 114.4mV | 117.1mV | 95.9mV | 135.6mV |
| ASDPP (filtered) | 22.9mV | 22.9mV | 22.0mV | 23.8mV | 18.7mV | 27.2mV |
| Effect of filtering | -79.89% | -80.53% | -80.77% | -79.68% | -80.50% | -79.94% |
| CASD | 232.9mV | 266.6mV | 262.6mV | 239.4mV | 96.7mV | 143.1mV |
| CASD (filtered) | 203.6mV | 239.6mV | 236.4mV | 209.6mV | 21.7mV | 53.3mV |
| Effect of filtering | -12.58% | -10.13% | -9.98% | -14.22% | -77.56% | -62.75% |

Statistical characteristics, including mean, average standard deviation per period (ASDPP) and cumulative average standard deviation (CASD)

much. The same is true for the white category. What the overall small filtered black ans white CASD values mean is that there is not much information lost when the material compositions and finishes of the samples are not taken into account. This implies that these latter factors do not significantly affect the results.

Signals in the acrylic and silicone categories have very similar statistical characteristics. Although their means are slightly different, this is less than half of their per-period average standard deviations (ASDPP). Moreover, the difference between signals produced by samples made of the same material cannot be overlooked, and filtering does not reduce the deviation by much when calculated cumulatively (CASD). These observations imply that the material composition of the sample does not significantly affect its reflectivity, and consequently its emissivity.

The remaining factor to be discussed is the finish of the samples. As seen from both the numerical (Table I) and graphical (second row of graphs in Figure 7) results, approximately the same can be said for the finish of the sample as its material composition, namely that it does not affect the signal much. This is an interesting consequence, as it goes against the notion that glossy and matte surfaces reflect light in fundamentally different ways, so materials with different finishes but otherwise identical parameters must have different reflectivity values. It is true in general that a matte surface reflects light differently than a glossy one. This difference, however, is not fundamentally in the amount of light reflected, but its direction. While the angle of incidence is always equal to the angle of reflection, the micro-scale plane corresponding to the reflection surface is not always identical to the macro-scale surface plane of the object. Glossy surfaces tend to be smoother on the micro-scale and therefore reflect a much higher proportion of the incoming light the same way as if the surface was modeled as a perfectly smooth plane. This way most incoming parallel light rays will remain parallel after reflection. This is called *specular reflection*. For matte surfaces, which have higher amounts of micro-scale surface irregularities the reflected light is much less directional. This is called *diffuse (Lambertian) reflection*, and it generally happens when the vertical scale of micro-scale surface deformities is higher than the wavelength of the incident light. Therefore, considering the samples with different finishes but otherwise identical parameters (such as in our experiment) will result in

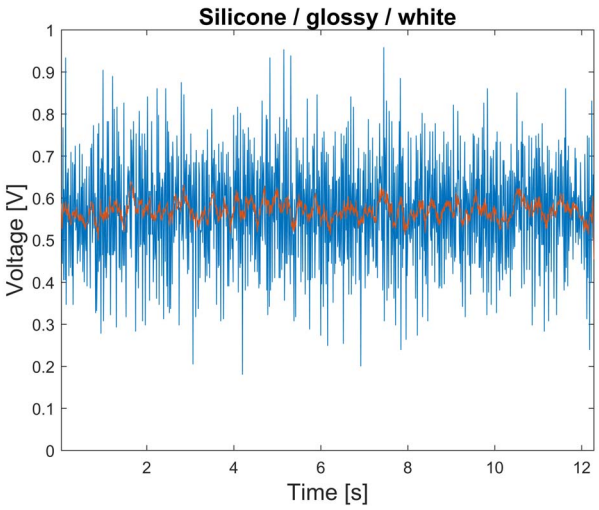


Fig. 5. A sample result of data collection for the white glossy silicone object. The blue line indicates the raw data while the red line is the smoothed data.

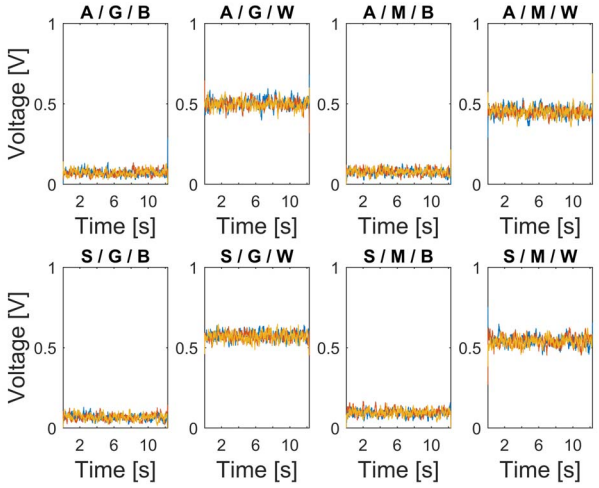


Fig. 6. Time-domain results for all 3 periods (blue, red and yellow) of all 8 samples smoothed with a moving average filter of length 11. The categories are: A (acrylic), S (silicone), G (glossy), M (matte), B (black) and W (white).

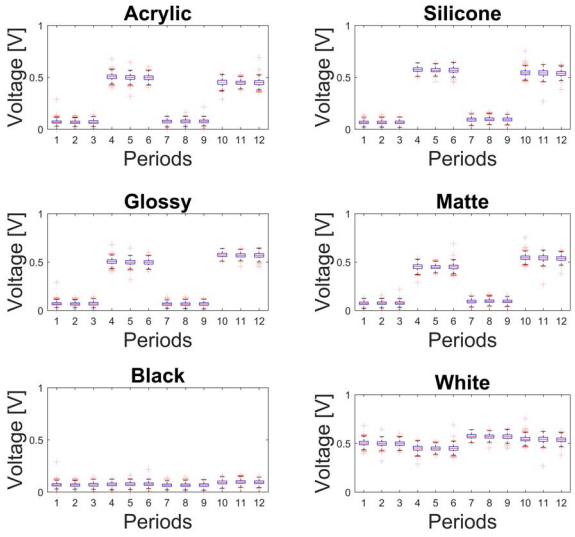


Fig. 7. Box plots of filtered results per category.

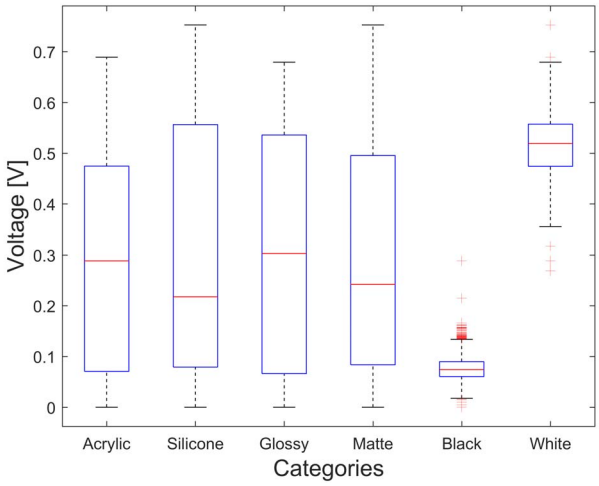


Fig. 8. Box plots of all categories.

different *directional reflectivity* distributions, but equal *hemispherical reflectivity* values. In our experiment, we use an array of LED lights, from which light arrives at the surface of the samples at different angles. Given the Helmholtz reciprocity [32], which states that a ray of light and its reverse go through identical optical effects in ordinary conditions (linear, stationary, non-magnetic medium), measuring the reflection of light from surrounding sources on an object at an angle that is perpendicular to its surface is equivalent to measuring the total hemispherical reflection of the object from a source that shines a beam that is perpendicular to the object's surface, which is its hemispherical exitance. Therefore in this experiment we are comparing hemispherical exitance values, which are theoretically identical for all kinds of finishes. This is why samples with both the glossy and the matte finishes are expected to produce values that are close to each other, and this experiment confirms the theory.

Finally, it is worth mentioning the quantitative aspects of the results. This paper does not present numerical emissivity estimations for these samples, which is due to lack of access to a way to obtain the real emissivity values of the samples. However, based on some trivial assumptions (such that transmittivity of each sample is negligible and that they reach steady state almost immediately i.e. the LED lights produce negligible heating) it is clear that for the same setup, the sensor reading will be linearly related to the emissivity: $V = c \cdot (1 - E)$, where $V$ is the voltage output, $E$ is the emissivity of the material and $c$ is a constant. The value of $c$ can be determined through calibration by performing

linear regression on data obtained from at least 2 objects with known (and different) emissivity values. Therefore the system is indeed capable of emissivity estimation.

## VI. Conclusion and Future Work

This paper detailed a system that is meant to complement thermography setups for characterization of materials through their thermal signatures. In order to perform quantitative analysis on the footage captured by thermal cameras, the emissivity value of the object under examination has to be accurately known, but different objects may have different emissivity values. The proposed system is capable of emissivity estimation in soft-real time, and in a contactless fashion. As a result, this system can serve as a building block for a fully functional thermographic material characterization system. Our future work includes improving the presented approach, testing it on a larger range of objects as well as integrating it into a circuit together with a laser source and a thermal camera to realize a thermographic material characterization system mentioned above.

## References


[1] Aujeszky, T., Korres, G., Eid, M.: Measurement-Based Thermal Modeling Using Laser Thermography. In: IEEE Transactions on Instrumentation and Measurement (2017).

[2] Aujeszky, T., Korres, G., Eid, M.: Thermography-based Material Classification using Machine Learning. In: IEEE International Sumposium on Haptic Audio-Visual Environments and Games (2017).

[3] Aujeszky, T., Korres, G., Eid, M.: Material Classification With Laser Thermography and Machine Learning. In: Quantitative InfraRed Thermography Journal (2018).

[4] Planck's radiation law — physics — Britannica.com https://www.britannica.com/science/Plancks-radiation-law

[5] Measuring Emissivity — Transcat http://www.transcat.com/calibration-resources/application-notes/measuring-emissivity/

[6] Calculating Emissivity https://www.optotherm.com/emiss-calculating.htm

[7] Kirchhoff's Law and Emissivity https://spie.org/publications/tt48_154_kirchhoffs_law_and_emissivity?SSO=1

[8] Q. Wang, P. Li, W. Zuo, and L. Zhang, *RAID-G: Robust estimation of approximate infinite dimensional Gaussian with application to material recognition*, Proceedings of the IEEE Conference on Computer Vision and Pattern Recognition, Jun. 2016, pp. 44334441.

[9] M. Brando, Y. M. Shiguematsu, K. Hashimoto, and A. Takanishi, *Material recognition CNNs and hierarchical planning for biped robot locomotion on slippery terrain* Proceedings of the IEEE-RAS 16th International Conference on Humanoid Robots (Humanoids), Nov. 2016, pp. 8188.

[10] T. Bhattacharjee, J. Wade, and C. Kemp, *Material recognition from heat transfer given varying initial conditions and short-duration contact* Proceedings of Robotics: Science and Systems, 2015, pp. 1927.

[11] S. Baglio, L. Cantelli, F. Giusa and G. Muscato, *Intelligent Prodder: Implementation of Measurement Methodologies for Material Recognition and Classification With Humanitarian Demining Applications*, IEEE Transactions on Instrumentation and Measurement, vol. 64, no. 8, pp. 2217-2226, Aug. 2015.

[12] T. Kakuda, A. Limarga, A. Vaidya, A. Kulkarni, and T. D. Bennett, *Non-destructive thermal property measurement of an APS TBC on an intact turbine blade*, Surface & Coating Technology, vol. 205, no. 2, 2010, pp. 446-451.

[13] P. Bison, F. Cernushi, and S. Capelli, *A thermographic technique for the simultaneous estimation of in-plane and in-depth thermal diffusivities of TBCs*, Surface & Coatings Technology, vol. 205, no. 10, 2011, pp. 3128-3133.

[14] I. Plotog, B. Mihailescu, I. Pencea, M. Branzei, P. Svasta, T. Cucu, and M. Tarcolea, *Methods for Pads Thermophysical Parameters Assessment in Terms of 4P Soldering Model*, IEEE 34th International Spring Seminar on Electronics Technology, 2011, pp. 320-326.

[15] N. Horny, J.-F. Henry, S. Offerman, C. Bissieux, and J. L. Beaudoin *Photothermal infrared thermography applied to the identification of thin layer thermophysical properties*, https://www.researchgate.net/publication/265667818, Retrieved February 15, 2019.

[16] N. W. Pech-May, A. Oleaga, A. Mendioroz, and A. Salazar, *Fast Characterization of the Width of Vertical Cracks Using Pulsed Laser Spot Infrared Thermography*, Journal for Nondestructive Evaluation, vol. 35, article 22, 2016.

[17] S. E. Burrows, A. Rashed, D. P. Almond, and S. Dixon, *Combined laser spot imaging thermography and ultrasonic measurements for crack detection*, Nondestructive Testing and Evaluation, vol. 22, 2007, pp. 217-227.

[18] K. Mouhoubi, J.-L. Bodnar, V. Detalle, and J.-M. Vallet, *Non-destructive testing of works of art by stimulated by infrared thermography: PPT interest*, Quantitative Infrared Thermography Conference (QIRT 16), 2016, pp. 144-151.

[19] J.-L. Bodnar, J.-L. Nicolas, K. Mouhoubi, J. C. Candore, and V. Detalle, *Characterization of an Inclusion of Plastazote Located in an Academic Fresco by Photothermal Thermography*, International Journal of Thermophysics, vol. 34, no. 8-9, 2013, pp. 1633-1637.

[20] S. Huth, O. Breitenstein, A. Huber, D. Dantz, U. Lambert, and F. Altmann, *Lock-in IR-Thermography a novel tool for material and device characterization*, Diffusion And Defect Data Part B Solid State Phenomena, vols. 82-84, 2002, pp. 741-746.

[21] P. E. Raad, P. L. Komarov, and M. G. Burzo, *Non-Contact Surface Temperature Measurements Coupled with Ultrafast Real-Time Computation*, Twenty-Third Annual IEEE Semiconductor Thermal Measurement and Management Symposium, 2007, pp. 57-63.

[22] C. Ionescu, M. Branzei, B. Mihailescu, and D. Bonfert, *Studies on Thermal Properties of Substrates for Electronics using IR Thermography*, IEEE 20th International Symposium for Design and Technology in Electronic Packaging (SIITME), 2014, pp. 45-49.

[23] *Heat Conduction Equation*, Wolfram Mathworld, http://mathworld.wolfram.com/HeatConductionEquation.html Retrieved February 18, 2019.

[24] N. W. Pech-May, N. Wilbur, A. Mendioroz, and A. Salazar, *Simultaneous measurement of the in-plane and in-depth thermal diffusivity of solids using pulsed infrared thermography with focused illumination*, NDT & E International, vol. 77, 2016, pp. 28-34.

[25] S. N. Pandya, B. J. Peterson, R. Sano, K. Mukai, E. A. Drapiko, A. G. Alekseyev, T. Akiyama, M. Itomi, and T. Watanabe, *Calibration of a thin metal foil for infrared imaging video bolometer to estimate the spatial variation of thermal diffusivity using a photo-thermal technique*, Review of Scientific Instruments, vol. 85, article 054902, 2014, pp. 1-9.

[26] T. Gfroerer, R. Phillips, and P. Rossi, *Thermal diffusivity imaging*, American Journal of Physics, vol. 83, 2015, pp. 923-927.

[27] L. Yeshurun and H. Azhari, *Non-invasive Measurement of Thermal Diffusivity Using High-Intensity Focused Ultrasound and Through-Transmission Ultrasonic Imaging*, Ultrasound in Medicine & Biology, vol. 42, no. 1, 2016, pp. 243-256.

[28] How to Measure the Unknown Thermal Emissivity of Objects/Materials Using the U5855A TrueIR Thermal Imager https://literature.cdn.keysight.com/litweb/pdf/5992-0222EN.pdf

[29] Usamentiage, R., Garcia, D. F., et al.: Temperature Measurement Using the Wedge Method: Comparison and Application to Emissivity Estimation and Compensation. In: IEEE Transactions on Instrumentation and Measurement (2011). Volume 60, Issue 5, pp 1768-1778.

[30] Iino, A., Tsukamoto, K. and Kusakabe, M.: Estimation of radiant temperature and emissivity of automobile's surface using infrared thermography. In: SICE 2003 Annual Conference (2003). ISBN: 0-7803-8352-4

[31] Fu, L., Fu, J., et al.: Spectral emissivity estimation based on K means clustering RBF neural network. In: 29th Chinese Control And Decision Conference (CCDC), 2017. pp. 7639-7642.

[32] Helmholtz reciprocity: its validity and application to reflectometry https://www.researchgate.net/publication/258169051_Helmholtz_Reciprocity_its_validity_and_application_to_reflectometry